

Relativistic transformations of quasi-monochromatic optical beams

Murat Yessenov and Ayman F. Abouraddy

CREOL, The College of Optics & Photonics, University of Central Florida, Orlando, FL 32816, USA

(Dated: August 10, 2022)

A monochromatic plane wave recorded by an observer moving with respect to the source undergoes a Doppler shift and spatial aberration. We investigate here the transformation undergone by a generic, paraxial, spectrally coherent quasi-monochromatic optical *beam* (of finite transverse width) when recorded by a moving detector. Because of the space-time coupling engendered by the Lorentz transformation, the monochromatic beam is converted into a propagation-invariant pulsed beam traveling at a group velocity equal to that of the relative motion, and which belongs to the recently studied family of ‘space-time wave packets’. We show that the predicted transformation from a quasi-monochromatic beam to a pulsed wave packet can be observed even at terrestrial speeds.

An observer moving with respect to an optical source emitting a monochromatic plane wave (MPW) records a Doppler-shifted MPW [1–4]. What are the changes observed by a detector moving with respect to a source emitting instead a generic monochromatic optical *beam* (i.e., a transversely localized field)? Previously tackled questions regarding relativistic transformations of optical fields have sometimes revealed surprising answers. For example, Terrell [5] and Penrose [6] showed that the length of an object in an image captured by an instantaneous shutter does *not* depend on the observer’s velocity, thus disabusing the physics community of the notion of a ‘visible’ Lorentz contraction [7]. Recently, it has been shown that angular-momentum carrying optical fields exhibit exotic effects in a frame moving orthogonally to the optical axis, including an optical analog of the relativistic spin Hall effect [8, 9], transverse orbital angular momentum and spatio-temporal vortices [10, 11], and relativistic spin-orbit interactions [12].

We analyze here the transformation of a generic quasi-monochromatic beam when recorded by an observer moving with respect to the source along the beam axis. Previous studies of such a transformation have revealed several mathematical results, the central one of which is that a strictly *monochromatic* beam is recorded as a finite-bandwidth *pulsed* beam [13–16]. The space-time coupling engendered by the Lorentz transformation yields a propagation-invariant wave packet whose group velocity is the relative velocity between source and detector [15]. Remarkably, the observed wave packet is a realization of so-called ‘space-time wave packets’ (STWPs) [17–22], which have been recently synthesized via spatio-temporal spectral-phase modulation [23–26].

Here we examine Lorentz transformations of spectrally coherent quasi-monochromatic optical beams, and provide an physically intuitive picture that underpins their conversion into STWPs. In this picture, an angularly induced Doppler broadening leads to the formation of an STWP, and we emphasize the impact of the beam’s spatial width on the induced spatio-temporal field structure. Crucially, by relaxing the ideal monochromaticity assumption, we find that the spectral linewidth of the source determines a minimum observer velocity for these effects to be detectable. We examine the potential for

observing such effects at terrestrial speeds with currently available narrow-linewidth lasers.

To set the stage for analyzing the Lorentz transformation of optical beams, we first examine the case of MPWs in one transverse dimension x (without loss of generality); see Fig. 1. An MPW at frequency ω emitted by a source \mathcal{S} at rest in the inertial frame $\mathcal{O}(x, z, t)$ is Doppler-shifted to $\omega' = \sqrt{\frac{1-\beta}{1+\beta}}\omega$ in the frame $\mathcal{O}'(x', z', t')$ moving at a velocity $v = \beta c$ along the common z -axis [Fig. 1(a)]. An MPW travelling in \mathcal{O} at an angle φ with the z -axis is transformed in \mathcal{O}' to a frequency $\omega' = \gamma(1 - \beta \cos \varphi)\omega$ travelling at an angle $\varphi' = \cos^{-1} \left[\frac{\cos \varphi - \beta}{1 - \beta \cos \varphi} \right]$ (the Doppler spatial aberration [3]), where $\gamma = 1/\sqrt{1 - \beta^2}$ [Fig. 1(b)].

These changes can be visualized on the surface of the spectral light-cone [22, 27]. The wave vector $\vec{k} = (k_x, k_z)$ for an MPW in \mathcal{O} is represented by a point on the surface $k_x^2 + k_z^2 = (\frac{\omega}{c})^2$, where $k_x = \frac{\omega}{c} \sin \varphi$ and $k_z = \frac{\omega}{c} \cos \varphi$.

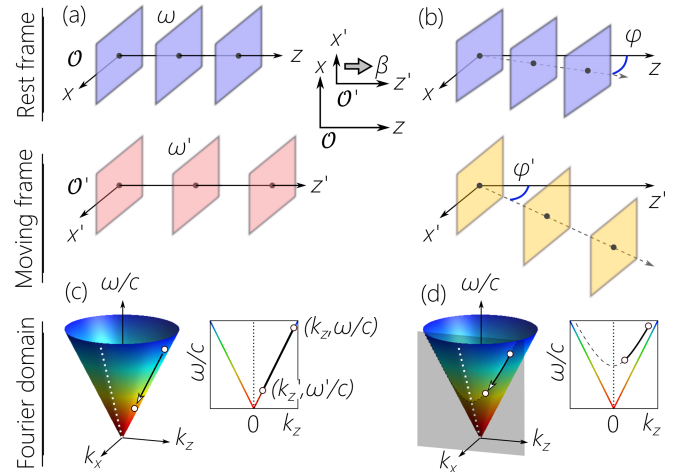


FIG. 1. A monochromatic plane wave (MPW) emitted in the rest frame \mathcal{O} is Doppler-shifted in the frame \mathcal{O}' moving along the $+z$ -axis. (b) An off-axis MPW in \mathcal{O} is Doppler-shifted and undergoes an angular rotation in \mathcal{O}' . (c) The on-axis MPW is Doppler-shifted along the light line $k_z = \omega/c$ ($k_x = 0$) in the Fourier domain, whereas (d) an off-axis MPW is shifted along a fixed- k_x hyperbola on the light-cone surface.

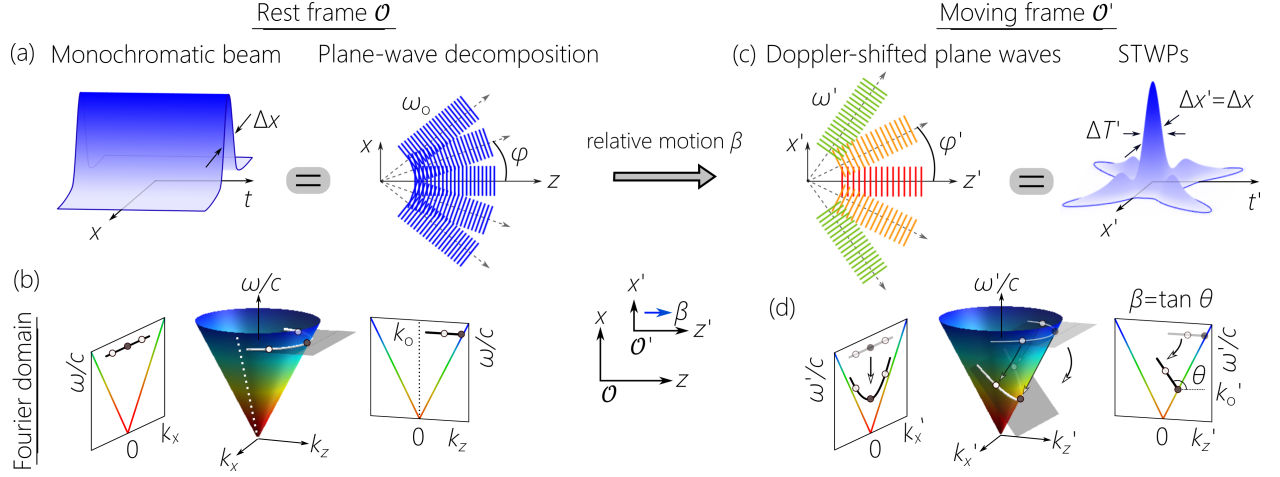


FIG. 2. Lorentz transformation of a monochromatic beam. (a) A monochromatic beam in \mathcal{O} is a superposition of plane waves of the *same* frequency ω_o travelling in *different* directions, and (b) its spectral support on the light-cone is an iso-frequency circle. (c) In the moving frame \mathcal{O}' , each plane wave undergoes an angle-dependent Doppler shift. (d) The spectral support for the field in (c) is the intersection of the light-cone with a plane that makes an angle θ with the k'_z -axis.

The Lorentz-transformed wave-vector components are: $k'_x = k_x$; $k'_z = \gamma(k_z - \beta\omega/c)$; and $\omega' = \gamma(\omega - c\beta k_z)$. Because $k_x'^2 + k_z'^2 = (\omega'/c)^2$, the structure of the light-cone itself is Lorentz invariant, so that the points corresponding to MPWs in \mathcal{O} and \mathcal{O}' can be represented on the same surface. The MPW in Fig. 1(a) corresponds to a point on the light-line $k_x = 0$, along which its Doppler-shifted counterpart in \mathcal{O}' is displaced [Fig. 1(c)]. In contrast, the point representing the off-axis MPW in \mathcal{O} [Fig. 1(b)] is displaced in \mathcal{O}' along a constant- k_x hyperbola [Fig. 1(d)].

Now consider a generic monochromatic *beam* emitted by the source \mathcal{S} in \mathcal{O} [Fig. 2(a)], which is a superposition of plane waves (spatial bandwidth Δk_x , inverse of the beam width Δx) all at the same frequency ω_o but traveling at different angles φ with the z -axis [28, 29]. The spectral support for such a beam is the circle $k_x^2 + k_z^2 = k_o^2$ at the intersection of the light-cone with a horizontal iso-frequency plane $\omega = \omega_o$ [Fig. 2(b)]; here $k_o = \omega_o/c$. Because the Doppler shift depends on the relative velocity v and angle φ between source and detector, the MPWs in \mathcal{O} undergo *different* Doppler shifts in \mathcal{O}' [Fig. 2(c)], and the associated points along the circle on the light-cone in \mathcal{O} are displaced in \mathcal{O}' differently along the constant- k_x hyperbolas [Fig. 2(d)]. Consequently, a finite spectral bandwidth $\Delta\omega'$ is Doppler-induced in the initially monochromatic beam, whose coherence guarantees that the space-time-coupled field in \mathcal{O}' is *pulsed* [Fig. 2(c)]. The spectral support is Lorentz-transformed from a horizontal circle in \mathcal{O} into a tilted ellipse in \mathcal{O}' [15] at the intersection of the light-cone with the plane $k'_z - k'_o = (\omega' - \omega'_o)c \tan \theta$, which is parallel to the k_x -axis but makes an angle θ with the k'_z -axis, where $\tan \theta = -\beta$ [Fig. 2(d)]. The linear relationship between k'_z and ω' indicates the absence of dispersion in the observed wave packet, which travels in \mathcal{O}' rigidly without diffraction at a group velocity $\tilde{v} = c \tan \theta = -v$ [22–24]. Such a field corresponds to a so-

called subluminal ‘baseband’ STWP [22, 23, 26], which have been recently synthesized with group velocities in the range $0.07c < \tilde{v} < c$ [24, 30, 31]. It will of course be challenging to produce such STWPs via relative motion between the source and detector.

In the paraxial regime $\Delta k_x \ll k_o$, the ellipse in \mathcal{O}' can be approximated [23] by a parabola $\Omega'(k'_x) = \frac{ck_x'^2}{2k_o'(1 - \cot \theta)}$ [Fig. 3(a)], where $\Omega' = \omega' - \omega'_o$. The initially monochromatic beam acquires a bandwidth $\Delta\Omega' = \frac{1}{2}\gamma|\beta|\omega_o(\frac{\Delta k_x}{k_o})^2$ via space-time coupling. Although $\Delta\Omega'$ is independent of the sign of β (i.e., it is symmetric with respect to approaching or receding observers), the carrier frequency ω'_o in contrast is highly asymmetric around $\beta = 0$ [Fig. 3(b)]. The resulting on-axis ($x = 0$) pulsewidth is $\Delta T' \sim \frac{1}{\gamma} \frac{z_R}{v}$, where z_R is the Rayleigh range of the initial monochromatic beam. At a wavelength $\lambda_o = 800$ nm and beam width $\Delta x = 40$ μm ($z_R \sim 1.6$ mm), relative motion at $v = 0.8c$ results in $\Delta T' \sim 4$ ps (a bandwidth $\Delta\lambda' \sim 0.25$ nm). The pulsewidth is reduced to $\Delta T \sim 250$ fs when the beam

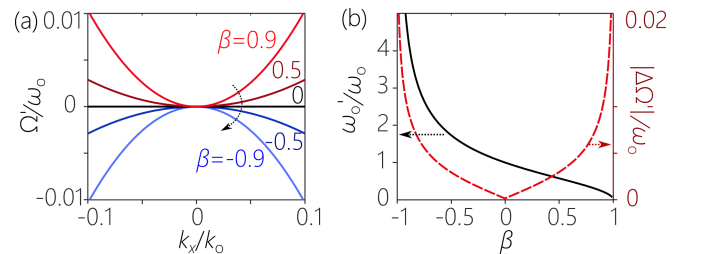


FIG. 3. (a) Spatio-temporal spectrum of paraxial STWPs in \mathcal{O}' for different observer velocities β . (b) Dependence of the STWP central frequency ω'_o (black solid curve, left axis) and bandwidth $|\Delta\Omega'|$ (red dashed curve, right axis) on β , normalized to the frequency ω_o of the monochromatic beam in \mathcal{O} having $\Delta k_x = 0.1k_o$.

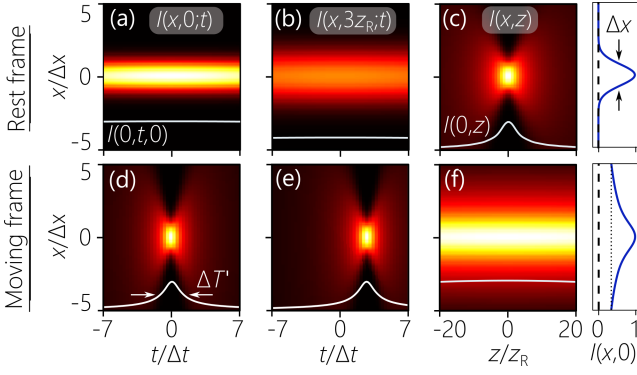


FIG. 4. (a) Spatio-temporal intensity profile $I(x, z; t)$ at the axial plane $z=0$ and (b) at $z=3z_R$ in the rest frame \mathcal{O} . (c) The time-averaged intensity $I(x, z)$ in \mathcal{O} . (d) Spatio-temporal intensity profile $I(x', z'; t')$ at $z'=0$ and (e) at $z'=3z_R$ in \mathcal{O}' . (f) The time-averaged intensity $I(x', z')$ in \mathcal{O}' .

width is reduced to $\Delta x = 10 \mu\text{m}$ ($\Delta\lambda \sim 4 \text{ nm}$).

Crucially, these conclusions are independent of the particular beam structure. In general, for a paraxial field $E(x, z; t) = e^{i(k_0 z - \omega_0 t)} \psi(x, z; t)$, the envelope is $\psi(x, z; t) = \iint dk_x d\omega \tilde{\psi}(k_x, \omega) e^{i(k_x x + (k_z - k_0)z - \omega t)}$. As a generic example, the spatio-temporal spectrum of a monochromatic Gaussian beam at ω_0 in the stationary frame \mathcal{O} is $\tilde{\psi}(k_x, \omega) = \tilde{\psi}(k_x) \delta(\omega - \omega_0)$, with $\tilde{\psi}(k_x) \propto \exp\{-\frac{k_x^2}{2(\Delta k_x)^2}\}$, so that $\psi(x, z; t) = \psi(x, z; 0)$. The time-resolved intensity $I(x, z; t) = |E(x, z; t)|^2$ at any axial plane z is thus independent of time [Fig. 4(a,b)]. Consequently, a ‘fast’ detector recording $I(x, z; t)$ or a ‘slow’ detector capturing the time-averaged intensity $I(x, z) = \int dt I(x, z; t)$ both reveal the *same* spatial Gaussian envelope in \mathcal{O} [Fig. 4(c)].

In the moving frame \mathcal{O}' , the spectrum is transformed into $\tilde{\psi}(k'_x, \omega') = \tilde{\psi}(k'_x) \delta(\Omega' - \Omega'(k'_x))$, from which it is straightforward to show that the envelope is propagation invariant $\psi(x', z'; t') = \psi(x', 0; t' - z'/\tilde{v}) = \psi(x', z' - \tilde{v}t'; 0)$, with $\tilde{v} = c \tan \theta = -v$. In other words, the roles of time and the axial coordinate z'/\tilde{v} are interchanged: the spatial profile observed along z for a monochromatic beam in \mathcal{O} [Fig. 4(c)] is now observed in time at a fixed axial plane in \mathcal{O}' [Fig. 4(d,e)]. This phenomenon was predicted in [13] where it was called ‘diffraction in time’ (which is distinct from ‘time-diffraction’ [32–34]) and verified experimentally in [15]. The invariance of k_x in frames moving along z guarantees that Δx remains invariant. The time-averaged intensity $I(x', z') = I_o + I_{\text{ST}}(x')$ [35] is now independent of z' and takes the form of a constant pedestal I_o atop of which is a Gaussian profile $I_{\text{ST}}(x') = \int dk'_x |\tilde{\psi}(k'_x)|^2 e^{i2k'_x x'}$ [Fig. 4(f)].

Recently, STWPs have been synthesized in the laboratory with $\tilde{v} \sim c$ starting with generic pulsed beams [26]. We inquire here whether relative motion at terrestrial velocities $v \ll c$ between a quasi-monochromatic source and a detector can lead to the observation of ultra-slow STWPs. To investigate this possibility, we must first drop the assumption of a strictly monochromatic field,

for which any non-zero relative velocity can in principle lead to the formation of a detectable STWP via idealized space-time coupling $\delta(\Omega' - \Omega'(k'_x))$. Rather, a realistic finite-energy field is inevitably quasi-monochromatic, and hence possesses a finite linewidth $\delta\Omega$ in \mathcal{O} . When transformed in \mathcal{O}' into an STWP, the precise delta-function correlation $\delta(\Omega' - \Omega'(k'_x))$ is relaxed to $g(\Omega' - \Omega'(k'_x))$ [30, 35], where $g(\cdot)$ is a narrow spectral function whose width corresponds to a finite *spectral uncertainty* $\delta\Omega' = \gamma(1 - \beta)\delta\Omega$. The spectral uncertainty $\delta\Omega$ sets a minimum relative velocity v_{\min} between source and detector that is required for a detectable STWP:

$$v_{\min} \sim 2c \left(\frac{\delta\Omega}{\omega_0} \right) / \left(\frac{\Delta k_x}{k_0} \right)^2 = k_0 \frac{(\Delta x)^2}{\delta T} \sim \frac{z_R}{\delta T}, \quad (1)$$

where $\delta T \sim 1/\delta\Omega$ is the pulsewidth of the field in \mathcal{O} .

This minimal requirement on the relative velocity can be understood from several perspectives. The spectral uncertainty $\delta\Omega$ is the finite bandwidth of the spectral support for the quasi-monochromatic field on the light-cone surface [Fig. 2(b)]. The Doppler-induced bandwidth $\Delta\Omega'$ results in an on-axis pulsewidth $\Delta T' \sim \frac{1}{\Delta\Omega'}$ that is independent of the initial linewidth $\delta\Omega'$. For the relative motion to produce a detectable STWP, the spectral tilt angle θ must be sufficient for the new spectral support on the light-cone to be distinguishable from the initial spectrum. This requires that $\Delta\Omega'$ exceed the spectral uncertainty, $\Delta\Omega' > \delta\Omega'$, which sets a minimal spectral tilt angle, and hence a minimal relative velocity. A different perspective is gleaned from consideration of the maximum propagation distance of an STWP $L_{\max} \sim \frac{c}{\delta\Omega' |1 - \cot \theta|}$ [30, 35]. Observing the STWP in \mathcal{O}' requires that L_{\max} be larger than the axial pulse length $v\Delta T' = \frac{z_R}{\gamma}$, thereby leading to the result in Eq. 1.

We illustrate in Fig. 5 the consequences of Eq. 1 starting with a quasi-monochromatic beam of $\frac{1}{e}$ -width $\Delta x = 100 \mu\text{m}$ (Rayleigh range $z_R \approx 5 \text{ mm}$) and spectral linewidth $\frac{\delta\Omega}{2\pi} = 300 \text{ Hz}$ ($\delta T = 1 \text{ ms}$ in \mathcal{O}) centered at $\frac{\omega_0}{2\pi} = 200 \text{ THz}$ ($\lambda_0 \approx 1.55 \mu\text{m}$) [Fig. 5(a)], which is observed by a moving detector [Fig. 5(b-e)]. From Eq. 1, $\beta_{\min} = 1.3 \times 10^{-7}$ or $v_{\min} \approx 140 \text{ km/h}$, so that an observer at $v = -5 \text{ km/h}$ ($|v| < v_{\min}$) records a conventionally diffracting quasi-monochromatic beam [Fig. 5(b)]. However, an observer at $v = -320 \text{ km/h}$ ($|v| > v_{\min}$) records an STWP with $\Delta T' \sim 0.5 \text{ ms}$, $L_{\max} \approx 10 \text{ mm}$, and $\tilde{v} = 320 \text{ km/h}$ [Fig. 5(c)]. An even faster observer moving at $v = -1600 \text{ km/h}$ detects an STWP of shorter pulsewidth $\Delta T' \sim 100 \mu\text{s}$ and longer propagation distance of $L_{\max} \approx 50 \text{ mm}$ [Fig. 5(d)].

Narrowing the linewidth to $\frac{\delta\Omega}{2\pi} = 3 \text{ Hz}$ reduces the threshold to $v_{\min} \approx 1.4 \text{ km/h}$, and recording an STWP becomes accessible to a walking observer, whereas the flying observer records an STWP travelling freely for $L_{\max} = 5 \text{ m}$. Alternatively, v_{\min} can be reduced more effectively by reducing the transverse beam width, due to the quadratic dependence $\beta_{\min} \propto (\Delta x)^2$.

We plot in Fig. 6 the on-axis intensity profiles $I(x' = 0, z'; t')$ with increasing v at $\frac{\delta\Omega}{2\pi} = 300 \text{ Hz}$, which can be

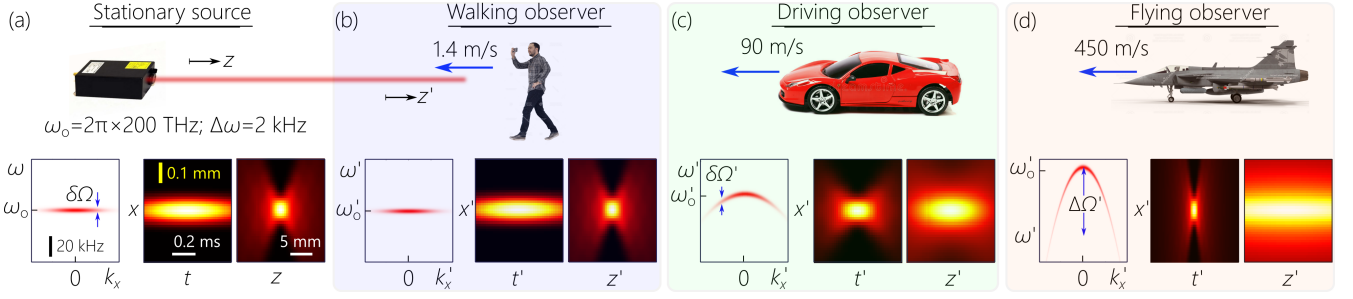


FIG. 5. Schematic of a potential test of relativistic transformations of a quasi-monochromatic beam. (a) A beam from a stationary laser ($\Delta x = 100 \mu\text{m}$, $\frac{\omega_o}{2\pi} = 200 \text{ THz}$, $\frac{\delta\Omega}{2\pi} = 300 \text{ Hz}$, and $z_R = 5 \text{ mm}$) is recorded by moving observers. (b) A walking observer at $v = -1.4 \text{ m/s}$ ($\approx 5 \text{ km/h}$) does *not* detect any change in the beam ($|v| < v_{\min} = 40 \text{ m/s}$). (c) A faster observer at $v = -90 \text{ m/s}$ ($\approx 320 \text{ km/h}$) detects a propagation-invariant STWP of pulsewidth $\Delta T' \approx 0.5 \text{ ms}$ traveling at a group velocity $\tilde{v} = 90 \text{ m/s}$, having a spatio-temporal spectral structure $\Omega' = \Omega'(k'_x)$. (d) An even faster observer at $v = -450 \text{ m/s}$ ($\approx 1600 \text{ km/h}$) observes an STWP of pulsewidth $\Delta T' \approx 0.1 \text{ ms}$.

viewed as world-lines for the peak of the pulsed field in \mathcal{O}' . In \mathcal{O} , the long temporal extent of $\sim 1 \text{ ms}$ (corresponding to a length of $\sim 300 \text{ km}$) combined with the short axial extent $\Delta z = 2z_R = 10 \text{ mm}$ renders the *peak* of the wave packet effectively ‘stationary’, even though the underlying electromagnetic field is travelling at c [Fig. 6(a)]. As the observer moves towards the source, the detected detected of the STWP can become significantly shorter than 1 ms when $v \gg v_{\min}$, resulting in an STWP peak moving at a group velocity $\tilde{v} = -v$ [Fig. 6(b-d)], and with the STWP propagation invariant within the temporal interval of 1 ms [Fig. 6(d)].

We have considered here a model in which the initial laser spectrum is coherent. However, the narrow-linewidth spectra of realistic laser sources are largely *incoherent*, corresponding to continuous-wave radiation rather than pulsed [36, 37]. The coherent spectral model utilized here can be obtained by modulating the narrow-linewidth source at a rate higher than its initial linewidth, resulting in a pulse train, each pulse of which is described by the model established here. The Lorentz transformation of a continuous-wave laser source with a spectrally incoherent narrow linewidth requires a different analysis [38, 39], which will be reported elsewhere. Furthermore, our analysis has been restricted to one transverse dimension, which has the advantage of showing a clear structure (the pedestal I_o) emerging as a result of space-time coupling. Incorporating both transverse dimensions in an azimuthally symmetric beam does not change the con-

clusions except that the pedestal is replaced with a slow $\frac{1}{r}$ -decay in intensity (r is the radial coordinate) [40, 41].

In contrast to previous tests of special relativity that rely on complex configurations and high-level precision [42–46], the conversion of a generic monochromatic paraxial beam into a propagation-invariant pulsed beam at terrestrial speeds is potentially simpler to realize, especially in light of the current availability of ultranarrow-linewidth lasers ($\frac{\delta\Omega}{2\pi} < 300 \text{ Hz}$) and high-speed cameras ($> 1000 \text{ frames/s}$). Although the Doppler shift is prohibitively difficult to detect at small β , the changes in the spatio-temporal structure of the field can be readily captured. Moreover, the results reported here may lead to new designs and functionalities for so-called space-time metasurfaces by elucidating what can be achieved at low-speed moving devices [47–50]. Other areas in optical physics have recently explored the ramifications of relativistic transformations of optical fields, including photonic time crystals [51, 52]; realizations of an optical analog of the Mackinnon wave packet [53] via moving dipoles [54, 55]; and reflection and refraction from moving surfaces [56–61]. Moreover, our findings may open a new perspective on transverse relativistic transformations of monochromatic beams carrying orbital angular momentum [8–12].

In summary, we have analyzed a generic quasi-monochromatic optical beam observed in an axially moving frame, showing that the transformed field is a propagation-invariant wave packet of finite pulsewidth travelling at subluminal group velocities. Moreover, an intuitive physical picture provides the constraint on the relative velocity between source and detector required to observe the predicted phenomena. Our analysis reveals that current technology allows for such a test to be carried out at terrestrial speeds.

Acknowledgments. Authors thank P. J. Delfyett, M. G. Vazimali and A. Duspayev for helpful discussions. This work was funded by the U.S. Office of Naval Research, contracts N00014-17-1-2458 and N00014-20-1-2789, and by the W. M. Keck Foundation.

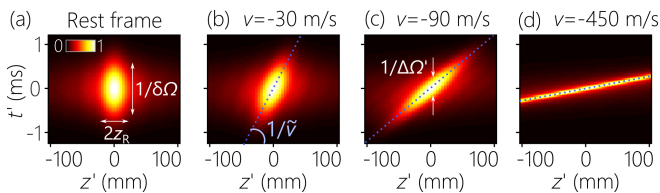


FIG. 6. On-axis intensity profile $I(x'=0, z'; t')$ of a $100\text{-}\mu\text{m}$ -wide beam and 1-ms pulse duration observed in \mathcal{O}' by (a) a stationary observer, or observers moving towards the source at (b) $v = -30 \text{ m/s}$, (c) -90 m/s , and (d) -450 m/s .

-
- [1] A. Einstein, On the electrodynamics of moving bodies, *Ann. Physik* **17**, 891 (1905).
- [2] D. Bohm, *The special theory of relativity* (Routledge, 2015).
- [3] E. F. Taylor and A. A. Wheeler, *Spacetime physics: Introduction to special relativity*, 2nd ed. (W.H. Freeman, 1992).
- [4] J. D. Jackson, *Classical Electrodynamics* (John Wiley & Sons, 1999).
- [5] J. Terrell, Invisibility of the Lorentz contraction, *Phys. Rev. Lett.* **116**, 1041 (1959).
- [6] R. Penrose, The apparent shape of a relativistically moving sphere, *Proc. Cambridge Phil. Soc* **55**, 137 (1959).
- [7] V. F. Weisskopf, The visual appearance of rapidly moving objects, *Phys. Today* **13**, 24 (1960).
- [8] K. Y. Bliokh and F. Nori, Relativistic Hall effect, *Phys. Rev. Lett.* **108**, 120403 (2012).
- [9] K. Y. Bliokh, Y. V. Izdebskaya, and F. Nori, Transverse relativistic effects in paraxial wave interference, *J. Opt.* **15**, 044003 (2013).
- [10] K. Y. Bliokh and F. Nori, Spatiotemporal vortex beams and angular momentum, *Phys. Rev. A* **86**, 033824 (2012).
- [11] K. Y. Bliokh, Spatiotemporal vortex pulses: Angular momenta and spin-orbit interaction, *Phys. Rev. Lett.* **126**, 243601 (2021).
- [12] D. A. Smirnova, V. M. Travin, K. Y. Bliokh, and F. Nori, Relativistic spin-orbit interactions of photons and electrons, *Phys. Rev. A* **97**, 043840 (2018).
- [13] S. Longhi, Gaussian pulsed beams with arbitrary speed, *Opt. Express* **12**, 935 (2004).
- [14] P. Saari and K. Reivelt, Generation and classification of localized waves by Lorentz transformations in Fourier space, *Phys. Rev. E* **69**, 036612 (2004).
- [15] H. E. Kondakci and A. F. Abouraddy, Airy wavepackets accelerating in space-time, *Phys. Rev. Lett.* **120**, 163901 (2018).
- [16] P. Saari and I. M. Besieris, Relativistic aberration and null Doppler shift within the framework of superluminal and subluminal nondiffracting waves, *J. Phys. Commun.* **4**, 105011 (2020).
- [17] H. E. Kondakci and A. F. Abouraddy, Diffraction-free pulsed optical beams via space-time correlations, *Opt. Express* **24**, 28659 (2016).
- [18] K. J. Parker and M. A. Alonso, The longitudinal isophase condition and needle pulses, *Opt. Express* **24**, 28669 (2016).
- [19] L. J. Wong and I. Kaminer, Ultrashort tilted-pulsefront pulses and nonparaxial tilted-phase-front beams, *ACS Photon.* **4**, 2257 (2017).
- [20] N. K. Efremidis, Spatiotemporal diffraction-free pulsed beams in free-space of the Airy and Bessel type, *Opt. Lett.* **42**, 5038 (2017).
- [21] M. A. Porras, Gaussian beams diffracting in time, *Opt. Lett.* **42**, 4679 (2017).
- [22] M. Yessenov, B. Bhaduri, H. E. Kondakci, and A. F. Abouraddy, Classification of propagation-invariant space-time light-sheets in free space: Theory and experiments, *Phys. Rev. A* **99**, 023856 (2019).
- [23] H. E. Kondakci and A. F. Abouraddy, Diffraction-free space-time beams, *Nat. Photon.* **11**, 733 (2017).
- [24] H. E. Kondakci and A. F. Abouraddy, Optical space-time wave packets of arbitrary group velocity in free space, *Nat. Commun.* **10**, 929 (2019).
- [25] B. Bhaduri, M. Yessenov, and A. F. Abouraddy, Anomalous refraction of optical space-time wave packets, *Nat. Photon.* **14**, 416 (2020).
- [26] M. Yessenov, A. A. Hall, K. L. Schepler, and A. F. Abouraddy, Space-time wave packets, *Adv. Opt. Photon.* **14**, 455 (2022).
- [27] R. Donnelly and R. W. Ziolkowski, Designing localized waves, *Proc. R. Soc. Lond. A* **440**, 541 (1993).
- [28] J. W. Goodman, *Fourier Optics* (Roberts & Company, 2005).
- [29] B. E. A. Saleh and M. C. Teich, *Principles of Photonics* (Wiley, 2007).
- [30] M. Yessenov, B. Bhaduri, L. Mach, D. Mardani, H. E. Kondakci, M. A. Alonso, G. A. Atia, and A. F. Abouraddy, What is the maximum differential group delay achievable by a space-time wave packet in free space?, *Opt. Express* **27**, 12443 (2019).
- [31] L. A. Hall and A. F. Abouraddy, Spectrally recycling space-time wave packets, *Phys. Rev. A* **103**, 023517 (2021).
- [32] M. Moshinsky, Diffraction in time, *Phys. Rev.* **88**, 625 (1952).
- [33] M. Moshinsky, Diffraction in time and the time-energy uncertainty relation, *Am. J. Phys.* **44**, 1037 (1976).
- [34] S. Godoy, Diffraction in time: Fraunhofer and Fresnel dispersion by a slit, *Phys. Rev. A* **65**, 042111 (2002).
- [35] H. E. Kondakci, M. A. Alonso, and A. F. Abouraddy, Classical entanglement underpins the propagation invariance of space-time wave packets, *Opt. Lett.* **44**, 2645 (2019).
- [36] C. H. Henry, Theory of the linewidth of semiconductor lasers, *IEEE J. Quantum Electron.* **18**, 259 (1982).
- [37] M. Pollnau and M. Eichhorn, Spectral coherence, Part I: Passive-resonator linewidth, fundamental laser linewidth, and Schawlow-Townes approximation, *Prog. Quantum Electron* **72**, 100255 (2020).
- [38] M. Yessenov, B. Bhaduri, H. E. Kondakci, M. Meem, R. Menon, and A. F. Abouraddy, Non-diffracting broadband incoherent space-time fields, *Optica* **6**, 522 (2019).
- [39] M. Yessenov and A. F. Abouraddy, Changing the speed of coherence in free space, *Opt. Lett.* **44**, 5125 (2019).
- [40] M. Yessenov, J. Free, Z. Chen, E. G. Johnson, M. P. J. Lavery, M. A. Alonso, and A. F. Abouraddy, Space-time wave packets localized in all dimensions, *Nat. Commun.* **13**, 4573 (2022).
- [41] K. Pang, K. Zou, H. Song, M. Karpov, M. Yessenov, Z. Zhao, A. Minoofar, R. Zhang, H. Song, H. Zhou, X. Su, N. Hu, T. J. Kippenberg, A. F. Abouraddy, M. Tur, and A. E. Willner, Synthesis of near-diffraction-free orbital-angular-momentum space-time wave packets having a controllable group velocity using frequency comb, *Opt. Express* **30**, 16712 (2022).
- [42] H. E. Ives and G. R. Stilwell, An experimental study of the rate of a moving atomic clock, *J. Opt. Soc. Am.* **28**, 215 (1938).
- [43] J. C. Hafele and R. E. Keating, Around-the-world atomic clocks: Observed relativistic time gains, *Science* **177**, 168 (1972).
- [44] R. Mansouri and R. U. Sexl, A test theory of special

- relativity: III. Second-order tests, *General relativity and Gravitation* **8**, 809 (1977).
- [45] P. Wolf, S. Bize, M. E. Tobar, F. Chapelet, A. Clairon, A. N. Luiten, and G. Santarelli, Recent experimental tests of special relativity, in *Special Relativity*, edited by J. Ehlers and C. Lämmerzahl (Springer, 2006) pp. 451–478.
 - [46] C. W. Chou, D. B. Hume, T. Rosenband, and D. J. Wineland, Optical clocks and relativity, *Science* **329**, 1630 (2010).
 - [47] Z. L. Deck-Léger, N. Chamanara, M. Skorobogatiy, M. G. Silveirinha, and C. Caloz, Uniform-velocity spacetime crystals, *Adv. Photon.* **1**, 056002 (2019).
 - [48] C. Caloz and Z.-L. Deck-Léger, Spacetime metamaterials—Part I: General, *IEEE Trans. Antennas Propag.* **68**, 1569 (2020).
 - [49] C. Caloz and Z.-L. Deck-Léger, Spacetime metamaterials—Part II: Theory and applications, *IEEE Trans. Antennas Propag.* **68**, 1583 (2020).
 - [50] P. Rocca, A. Alú, C. Caloz, and S. Yang, Guest editorial: Special cluster on space-time modulated antennas and materials, *IEEE Antennas Wirel. Propag. Lett.* **19**, 1838 (2020).
 - [51] M. Lyubarov, Y. Lumer, A. Dikopoltsev, E. Lustig, Y. Sharabi, and M. Segev, Amplified emission and lasing in photonic time crystals, *Science*, eabo3324.
 - [52] Y. Sharabi, A. Dikopoltsev, E. Lustig, Y. Lumer, and M. Segev, Spatiotemporal photonic crystals, *Optica* **9**, 585 (2022).
 - [53] L. Mackinnon, A nondispersive de Broglie wave packet, *Found. Phys.* **8**, 157 (1978).
 - [54] F. Wilczek, *A Beautiful Question: Finding Nature’s Deep Design* (Penguin Press, 2015).
 - [55] L. A. Hall and A. F. Abouraddy, Observation of optical de Broglie-Mackinnon wave packets, unpublished (2022).
 - [56] B. W. Plansinis, W. R. Donaldson, and G. P. Agrawal, What is the temporal analog of reflection and refraction of optical beams?, *Phys. Rev. Lett.* **115**, 183901 (2015).
 - [57] H. Qu, Z.-L. Deck-Léger, C. Caloz, and M. Skorobogatiy, Frequency generation in moving photonic crystals, *J. Opt. Soc. Am. B* **33**, 1616 (2016).
 - [58] B. W. Plansinis, W. R. Donaldson, and G. P. Agrawal, Temporal waveguides for optical pulses, *J. Opt. Soc. Am. B* **33**, 1112 (2016).
 - [59] B. W. Plansinis, W. R. Donaldson, and G. P. Agrawal, Single-pulse interference caused by temporal reflection at moving refractive-index boundaries, *J. Opt. Soc. Am. B* **34**, 2274 (2017).
 - [60] B. W. Plansinis, W. R. Donaldson, and G. P. Agrawal, Cross-phase-modulation-induced temporal reflection and waveguiding of optical pulses, *J. Opt. Soc. Am. B* **35**, 436 (2018).
 - [61] Z.-L. Deck-Léger, X. Zheng, and C. Caloz, Electromagnetic wave scattering from a moving medium with stationary interface across the interluminal regime, *Photonics* **8**, 202 (2021).